Dual-space analysis based on symmetries for phonons in AlAs/GaAs shell quantum dots

2002 J. Phys.: Condens. Matter 14 8771

(http://iopscience.iop.org/0953-8984/14/38/302)

INSTITUTE OF PHYSICS PUBLISHING JOURNAL OF PHYSICS: CONDENSED MATTER

J. Phys.: Condens. Matter **14** (2002) 8771–8786 PII: S0953-8984(02)35934-4

Dual-space analysis based on symmetries for phonons in AlAs/GaAs shell quantum dots

G Qin[1,3,4] **and S F Ren**[2]

[1] CCAST (World Laboratory), PO Box 8730, Beijing 100080, People's Republic of China
[2] Department of Physics, Illinois State University, Normal, IL 61790-4560, USA

E-mail: gqin@nju.edu.cn

Received 17 April 2002, in final form 31 July 2002
Published 12 September 2002
Online at stacks.iop.org/JPhysCM/14/8771

Abstract

Phonon modes in shell quantum dots (SQDs) composed of a spherical AlAs core embedded in a GaAs shell, with up to about 12 000 atoms (about 8.5 nm in outer diameter), are calculated by using a valence force field model. All the vibration frequencies and amplitudes are evaluated directly from the lattice dynamic matrix by employing the projection operators of the group theory. The numerous SQD phonon modes in each of five symmetries which suffer more quantum confinement than modes in a usual quantum dot owing to the small scale of the shell's thickness are classified by using an analysis method both in real space and in reciprocal space. It is found that the bulk GaAs-like SQD modes with localization radius located in the interior of the shell have clearly pronounced bulk specific $\boldsymbol{k}$-point parentage from a specific part of the Brillouin zone (BZ) (Γ derived, X derived etc) and from a definite bulk band (one of six modes). In AlAs/GaAs SQDs of all sizes, the bulk GaAs-LO(Γ)-like SQD modes always have A_1 symmetry, while the bulk GaAs-TO(Γ)-like and bulk-GaAs-A(Γ)-like dot modes have T_1 symmetry. The bulklike SQD mode of specific symmetry has a dominant BZ parentage peak around the bulk origins, so the frequencies of these SQD modes can be approximately related to a single bulk phonon band at a single wavevector $\boldsymbol{k}^*$. In addition to the frequencies of bulk GaAs-A(Γ)-like SQD modes blue-shifting as the shell's characteristic scale reduces, the bulk-GaAs-like Γ-derived LO and TO SQD modes red-shift in frequency with decreasing shell characteristic scale. There is almost no LO/TO mixing for bulklike modes. The identification and classification of SQD modes have fundamental importance in the discussion of the Raman spectrum and electron–phonon interaction.

[3] Author to whom any correspondence should be addressed.
[4] Home institution and mailing address: Department of Physics, Nanjing University, Nanjing 210093, People's Republic of China.

0953-8984/02/388771+16$30.00

1. Introduction

Semiconductor quantum dots (QDs) have attracted much research attention in recent years because of their importance in the fundamental understanding of physics and potential applications. Shell quantum dots (SQDs) that are composed of a spherical core of one material embedded in a matrix of another material, for example Mg/MgO, CdTe/CdO [1, 2], CdS/HgS, CdS/PbS, InAs/GaAs, GaAs/AlAs [3–6] and Si/SiO_2 [7], are of interest in optical absorption, polarons, visual PL phenomena and many other physical phenomena. They have displayed a variety of interesting properties, such as the quantum confinement of carriers, the increase of the absorption band edge and the control of the luminescence efficiency. Since 1993, a new class of QDs, called quantum-dot quantum wells (QDQWs), such as CdS/HgS/CdS, ZnS/CdSe/ZnS, CdS/PbS/CdS and InP/InAs/InP QDQWs, have been fabricated and studied [8–15]. They are composed of two semiconductor materials, of which the one with a smaller bulk bandgap is embedded between a core and an external shell of a second material with a large bulk bandgap, i.e., the QDs have a quantum well region inside, or they have an internal nanoheterostructure. Obviously, an SQD is only a special kind of QDQW with no external shell.

The electronic properties of these QD structures have been intensively studied in recent years, both theoretically and experimentally, and a clear understanding of much of the basic physics of the quantum confinement effects of electrons in them has been achieved [16]. On the other hand, the vibration properties of these QD structures, i.e., the confinement of phonon modes in them, are less understood. It is well known that the phonon-assisted carrier relaxations have significant influence on the photoluminescence in Si/SiO_2 SQDs [17]. By using hole burning (HB) and fluorescence line-narrowing (FLN) spectroscopy, in the study of optical absorption and emission in CdS/HgS/CdS QDQWs, Mews *et al* [10] found that the appearance of the side bands reflects the strong coupling of the electron excitation to LO phonons. Yeh *et al* [18] discussed the coupling of excitations to phonons in CdS/HgS/CdS QDQWs. They argued that the photo-induced exciton couples to the 300 cm^{-1} LO phonon mode and propose a model for the origin of the initial excitation. This means that the phonons and carrier–phonon interaction play an important role in the research of QD structures. So far, most of the theoretical understanding of phonon modes in QD structures is based on the continuum dielectric models and other phenomenological models [19]. The analytic expressions of the eigenfunctions of LO phonons and surface optical phonons of superlattices [20], multilayer structures [19] and small spherical [4, 5, 21–24] and cylindrical [25] QDs and SQDs [1] are derived and the electron–phonon interactions and Raman scattering [26] are calculated. However, one of the basic assumptions of all dielectric models is that the material is homogeneous, that is only valid in the long wavelength limit. When the size of QD structures is small, in the range of a few nanometres, the continuum dielectric models are intrinsically limited. Many optical, transport and thermal properties of QDs are related to phonon behaviour in QD structures. The theoretical treatment of these properties requires a reliable description of phonon modes and electron–phonon interaction potential in them.

Until now, we have rarely known any effort made in the microscopic modelling of the phonon modes in SQDs or QDQWs. Since most microscopic models can only handle QD structures with very small size (<45 Å in outer diameter), it is unrealistic to treat QDs with several different shells. In recent years, we have developed a microscopic valence force field model (VFFM) [27–30] to study phonon modes in QDs by employing the projection operators of the irreducible representations of the group theory to reduce the computational intensity. By employing the group theory, for example, the dynamic matrix of size 35 565 can be reduced to five matrices in five different representations of A_1, A_2, E, T_1 and T_2, with the sizes of 1592, 1368, 2960, 4335 and 4560 respectively. Therefore, the original problem is reduced

to a problem that can be easily handled by most reasonable computers. Not only does this allow the investigation of phonon modes in QD structures with a much larger size, but also it allows the investigation of phonon modes in these structures with different symmetries. These investigations lead to much interesting physics that otherwise cannot be revealed. With this model that will be mentioned as a VFFM model based on group theory later, we have studied the size effects of phonon modes in semiconductor QDs, including QDs of one material, such as GaAs [27] and InAs [28], and GaAs/AlAs SQDs with a GaAs core embedded in a shell of AlAs [29], as well as the size effect on Raman intensity of Si QDs [30].

After completing the calculation of phonons of QD structures, another challenging task is to classify the very numerous eigenmodes. A efficient dual-space analysis method suggested by Fu *et al* [31] is very useful for this purpose. In one of our previous articles [32], phonon structures of Si QDs with diameters up to 79 Å are calculated by employing the VFFM model. Then the large number of modes are classified and analysed by a improved dual-space analysis method based on the symmetrical character of group theory. It is found that phonon modes can be identified not only by their bulk parentages, but also by their symmetrical characters.

In this article, as a preliminary effort in the research of QDQWs, based on the same model, phonon modes in AlAs/GaAs SQDs, i.e., a core of barrier material AlAs (material with larger gap) of diameter d_S embedded in a shell of well material GaAs (material with smaller gap) of outer diameter d_L, are calculated and analysed by means of a dual-space analysis method based on symmetries. The significant difference between this calculation and that performed in [32] comes from the fact that unlike the Si atoms carrying zero effective charge, Ga, As and Al atoms have different nonzero effective charge, so attention must be paid to dealing with the charge effect of the AlAs/GaAs SQDs. AlAs/GaAs SQDs are much more important than GaAs/AlAs SQDs, since the shell material has a narrower energy gap than the core material, there is a quantum well region in it. It is a special case of AlAs/GaAs/AlAs QDQWs with zero thickness of outer AlAs shell. So the approaches used here are completely suitable to deal with other semiconductor QDs, SQDs and QDQWs with zinc-blende structure in which the ions carry some number of effective charges.

The article is organized as follows. In section 2, we describe the theoretical model of VFFM and the analysis approaches in dual space; in section 3, we show our calculated results and give some discussions; and section 4 is a summary.

2. The theoretical approaches

2.1. VFFM for phonon modes in QDs

The theoretical model we used to investigate phonon modes in QDs is a valence force field model (VFFM). In general, this model can be used to study phonon modes in group V, III–V and II–VI semiconductors. In this model, the change of the total energy due to the lattice vibration is considered as two parts, the change of the energy due to the short-range interactions and the change of the energy due to the long-range Coulomb interaction:

$$\Delta E = \Delta E_s + \Delta E_c \tag{1}$$

where the short-range interaction describes the covalent bonding, and the long-range part approximates the Coulomb interactions of polar semiconductor compounds. For the short-range part, we employed a VFFM with only two parameters as follows [33, 34]:

$$\Delta E_s = \sum_i \frac{1}{2} C_0 \left(\frac{\Delta d_i}{d_i} \right)^2 + \sum_j \frac{1}{2} C_1 (\Delta \theta_j)^2 \tag{2}$$

where C_0 and C_1 are two parameters describing the energy change due to the bond length change and the bond angle change respectively. The summation runs over all the bond lengths and bond angles. Because each of these two parameters has a simple and clear physical meaning, this model allows us to treat the interaction between atoms near and at the surface appropriately. It can be further used to treat the surface relaxations and reconstructions as well as the surface and interface strains without much difficulty. In general, for the long-range Coulomb interaction, we have

$$E_c = \frac{1}{2}\sum_{i\neq j}\frac{e_i^* e_j^*}{|r_{ij}|}, \tag{3}$$

where e^* is an effective charge introduced to describe the long-range Coulomb interaction [35], and $|r_{ij}|$ is the distance between two charges i and j. The parameters C_0, C_1 and e^* used in our calculations for GaAs are taken as 38.80, 0.858 and 0.6581 [33], and the calculated phonon frequencies of GaAs QDs agree reasonably well with the experimental data. For the core material AlAs, we have used two different sets of parameters in our calculation. The first set contains the same parameters as GaAs which results in the calculated longitudinal and transverse optical frequency of bulk AlAs at the Γ point, $\nu_{\mathrm{LO}}^{\mathrm{AlAs}}(\Gamma) = 11.8580$ and $\nu_{\mathrm{TO}}^{\mathrm{AlAs}}(\Gamma) = 10.9165$ THz, respectively. The second set of parameters, which is in fact the best set we have found in fitting the data, is that C_0, C_1 and e^* are equal to 39.15, 0.850 and 0.6581, respectively. The calculated results of using the second set are $\nu_{\mathrm{LO}}^{\mathrm{AlAs}}(\Gamma) = 11.8943$ and $\nu_{\mathrm{TO}}^{\mathrm{AlAs}}(\Gamma) = 10.9559$ THz, respectively, which are only slightly improved in fitting the experimental data of $\nu_{\mathrm{LO}}^{\mathrm{AlAs}}(\Gamma) = 12.1111$ and $\nu_{\mathrm{TO}}^{\mathrm{AlAs}}(\Gamma) = 10.851$ THz [36]. Our theoretical formalism has considered the detail of the interactions in SQDs; it can be used to deal with phonon modes in SQDs with different parameters for core and shell. However our results show that taking the above two different sets of parameters for AlAs produces qualitatively similar results for the AlAs/GaAs SQDs; for simplicity we present the results of the second set, i.e., taking GaAs parameters for both GaAs and AlAs and only considering the mass difference.

When considering the interaction between atoms, special attention is paid to atoms near the external surface of the GaAs shell as well as the interface between the AlAs core and the GaAs shell. More specifically, for the short-range interaction, when an atom is located near the surface, interaction from its nearest-neighbouring atom is considered only if that specific nearest atom is within the SQD, and interaction from its second-neighbouring atom is considered only if that specific second-neighbour atom is in the SQD as well as the nearest-neighbouring atom that connects them. The second point is important, because it makes sense with the physical meanings of these two parameters, but it is easy to neglect. Similar attention is paid to the atoms located near the interface of the core and shell. We have also paid attention to the long-range Coulomb interaction. We have used the same transfer charge for GaAs and AlAs since they are similar [35]. Because the total numbers of anions and cations in an SQD might not be the same, the entire SQD might not be neutral in electric charge in our model. Therefore, we performed our calculations based on two different approaches. In the first, we assumed that atoms at the surfaces carry the same charge as those in the bulk, and this is named the natural charge approach. In the second, we assumed that the surface atoms take the charge that makes the entire SQD neutral, and this charge might be slightly different from those in the bulk. The second one is named the neutral charge approach. Later we will show that our calculations indicate that these two approaches do not make a critical difference, and they give qualitatively similar results. Our results shown in this article are from the natural charge approach. As we discussed in the above section, we have employed the projection operators of the irreducible representations of the group theory to reduce the computational intensity [37, 38] when calculating phonon modes directly from the dynamic matrices. Not only is the original

problem reduced to a problem that can be easily handled by most reasonable computers, but also it allows us to investigate phonon modes with different symmetries in QDs which leads to much interesting physics [27–30]. When the results of phonon modes are used to calculate the electron–phonon interaction or Raman intensity of QDs, the advantage of applying the group theory to calculate phonon modes in different symmetries is even more obvious. For example, because of the symmetry dependence of Raman intensity, only phonon modes that are Raman active in that specific symmetry are necessary to consider. This dramatically reduces the amount of calculations in Raman intensity of QDs with microscopic models [30].

2.2. Dual-space approach for analysing dot phonon modes based on the symmetry of the group theory

An efficient method to analyse the characters of numerous phonon modes in QD or SQD is the dual-space approach, i.e., the modes are analysed both in the reciprocal space and in the real space [31].

In real space, we evaluate the localization radius for a normal mode λ defined as

$$R_\lambda^2 = \sum_l \left(\sum_{c=1}^{3} |a_{l,c}^\lambda|^2 \right) \boldsymbol{r}_l^2 \Big/ \left(\sum_l \sum_{c=1}^{3} |a_{l,c}^\lambda|^2 \right) \tag{4}$$

where $a_{l,c}^\lambda$ is the vibrational amplitude of the lth atom in the c direction ($c = x, y, z$) of the λ mode. $\boldsymbol{r}_l$ is the radial vector of the lth atom in the SQD relative to the centre of the SQD. $\lambda = (\alpha, j)$ is a mode index, where (α, j) means the jth phonon mode in the α irreducible representation (or symmetry). α should be one of the five irreducible representations, A_1, A_2, E, T_1 and T_2. R_λ tells us in what part of the SQD the mode's vibrational amplitude is localized. It is useful to distinguish modes which are localized in the interior of the core or the shell of the SQD ('bulklike modes') from those localized on the periphery of the core or the shell ('surface-like modes').

Another efficient way of analysing phonon modes in the SQD is establishing the relation between the SQD modes and the bulk modes, i.e., evaluating the k-space projection of the eigenstate of SQD mode λ to those of the six bulk modes of the core material or the shell material in reciprocal space. Suppose the eigenstates of the bulk phonon are expressed by $\chi_{n,\boldsymbol{k}}$ where $\boldsymbol{k}$ is the wavevector, $n = 1$–6 corresponding to six bulk phonon states, i.e., three acoustic modes (TA1, TA2 and LA) and three optical modes (TO1, TO2 and LO); the k-space projection of the dot's eigenstate ϕ_λ with $\lambda = (\alpha, j)$ to bulk states of the core material or the shell material is defined as

$$C_{n,\boldsymbol{k}}^\lambda = |\langle \chi_{n,\boldsymbol{k}}, \phi_\lambda \rangle|^2 = \frac{1}{N} \left| \sum_{l,m,c} (d_{m,c}^{n,\boldsymbol{k}})^* \cdot C_{l,c}^\lambda \exp[\mathrm{i}\boldsymbol{k}(\boldsymbol{r}_l - \boldsymbol{r}_m)] \right|^2 \tag{5}$$

where N is the total atomic number in the SQD. $\boldsymbol{r}_l$ and $\boldsymbol{r}_m$ are the radial vectors of the lth and the mth atoms. $m = 1$ or 2 corresponding to the first or second atom in each primitive cell. $c = x$, y and z, $d_{m,c}^{n,\boldsymbol{k}}$ and $C_{l,c}^\lambda$ are the expanding coefficients of bulk and dot eigenstates to vibrational eigenvectors, respectively.

Then in terms of equation (5), we may define the Brillouin-zone (BZ) parentage of an SQD mode λ as the contribution of the bulk eigenmodes with the wavevector length k in forming this SQD mode:

$$P_\lambda(k) = \int \mathrm{d}\boldsymbol{k}\, \delta(|\boldsymbol{k}| - k) \sum_n |C_{n,\boldsymbol{k}}^\lambda|^2. \tag{6}$$

This quantity tells us which part of the bulk BZ contributes to a given SQD eigenmode. Another quantity used is the bulk specific $\boldsymbol{k}$-point parentage T_λ measuring the extent to which the SQD

eigenmode is derived from the bulk states near the specific point in reciprocal space. The bulk Γ parentage is defined as

$$T_\lambda(n, \Gamma, K_{cut}) = \int_\Omega \mathrm{d}\boldsymbol{k}\, |C^\lambda_{n,\boldsymbol{k}}|^2 = \int_0^{K_{cut}} \mathrm{d}k \int \mathrm{d}\hat{\boldsymbol{k}}\, |C^\lambda_{n,\boldsymbol{k}}|^2 \tag{7}$$

where $\hat{\boldsymbol{k}}$ is the direction angle of wavevector $\boldsymbol{k}$. Typically, we choose K_{cut} as $2\sqrt{3}\pi/d$ which is determined by the first node $k = 2\pi/d$ of the Bessel function $j_0(kr)$ ($d = d_S$, the core diameter, for the core material and $d = d^*$, the shell's characteristic scale, for the shell material where $d^* = 2/(\frac{1}{d_L} + \frac{1}{\Delta d})$ with d_L and Δd the outer diameter and shell thickness of the shell). Finally, in order to investigate the possibility of mode mixing in SQDs, we evaluated also the bulk-band parentage of the SQD mode λ as

$$A_\lambda(n) = \int \mathrm{d}\boldsymbol{k}\, |C^\lambda_{n,\boldsymbol{k}}|^2; \tag{8}$$

we say that there is a mixing between two or more bulk modes when $A_\lambda(n)$ with $n = 1, 6$ has significant contributions from more than one bulk phonon band.

3. Results and discussions

First of all, we calculate the phonon modes in the AlAs/GaAs SQD which is composed of a spherical AlAs core of diameter d_s embedded in a GaAs shell of outer diameter d_L, so the thickness of the shell is $\Delta d/2$ with $\Delta d = d_L - d_S$ or the double thickness of the shell is Δd. The frequencies of phonon modes of AlAs/GaAs SQDs are calculated as a function of sizes (d_S and d_L) for each of five representations of A_1, A_2, E, T_1 and T_2. The results of our microscopic model show that the whole frequency region of optical modes is divided into two nonoverlapping bands, the upper band (AlAs-like band) and the lower band (GaAs-like band), originated from the bulk AlAs optical band and bulk GaAs optical band, respectively. The AlAs-like band is located inside the bulk AlAs optical band that covers the frequency range of $\nu_{\mathrm{TO}}^{\mathrm{AlAs}}(K) = 318.6198\ \mathrm{cm}^{-1} = 9.5586$ to $\omega_{\mathrm{LO}}^{\mathrm{AlAs}}(\Gamma) = 395.2666\ \mathrm{cm}^{-1} = 11.8580$ THz, respectively. The GaAs-like band is located inside the bulk GaAs optical band that covers the frequency range of $\nu_{\mathrm{TO}}^{\mathrm{GaAs}}(\Gamma) = 268.7981\ \mathrm{cm}^{-1} = 8.0639$ to $\nu_{\mathrm{LO}}^{\mathrm{GaAs}}(\Gamma) = 292.1294\ \mathrm{cm}^{-1} = 8.7639$ THz, respectively. All these results are in accord with those given by the dielectric continuum model [2, 3].

In the analysis of phonon modes below, we concentrate mainly on both bulk and surface GaAs-like phonon modes with frequencies in the GaAs-like band and localized mostly in the GaAs shell, not only because these phonon modes suffer a stronger quantum confinement effect than those in usual QDs caused by an internal quantum well of thickness $\Delta d/2$, but also because these modes have a more significant effect on the carriers localized mainly in the GaAs shell (or in the internal quantum well).

In the real space, the localization radius of all SQD modes and the densities of states (DOSs) are evaluated. We use the square of frequency, ν^2, as the x-axis scale in order to achieve higher resolution in the optical region. In all the figures through this article, the data of SQD modes of A_1, A_2, E, T_1 and T_2 symmetry are always plotted as open circles, solid squares, open up triangles, solid down triangles and open diamonds, respectively. The localization radii of phonon modes, R_λ, are plotted as a function of ν^2 in figure 1 for each of five symmetries in a 30/50 AlAs/GaAs SQD. For simplicity, from now on, an SQD of $d_S = 30$ Å and $d_L = 50$ Å is denoted as a 30/50 SQD. We can see from figure 1 that the localization radii of optical modes having frequencies in the AlAs-like phonon band is always no more than 30 Å, i.e., the AlAs-like modes are localized mainly in the AlAs core, while the localization radii of optical modes

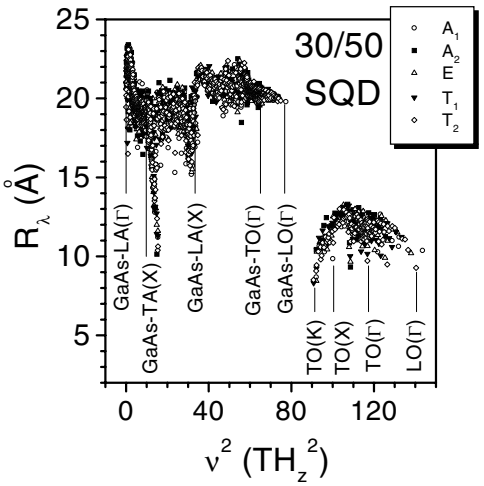

Figure 1. Localization radii of SQD modes of A_1, A_2, E, T_1 and T_2 symmetries in a 30/50 AlAs/GaAs SQD. The identities of highly localized modes with localization radii located in the interior of the shell or the core, LO(Γ)-like, TO(Γ)-like, LO(X)-like, TO(X)-like of bulk GaAs and bulk AlAs etc, are indicated by vertical lines.

having frequencies in the GaAs-like phonon band is not less than 30 Å, i.e., the GaAs-like modes are localized mainly in the GaAs shell. The identities of highly localized modes (with localization radii in the interior of the core or shell) are indicated by vertical lines. The vertical lines in the region of $\nu^2 \geqslant 91.3668\ \mathrm{THz}^2$ indicate the frequencies of bulk LO- and TO-phonon modes of AlAs, while those in the region of $\nu^2 \leqslant 76.8056\ \mathrm{THz}^2$ indicate values of GaAs. The SQD modes that have their localization radii in the shell's interior are 'bulk GaAs-like' (shell-interior modes), while others having localization radii inside and near both surfaces of the GaAs shell are surface GaAs-like modes. Similarly, SQD modes having their localization radii in the interior of the AlAs core are 'bulk AlAs-like' (core-interior modes), while others having localization radii inside the core and near the interface of the GaAs shell and AlAs core are interface AlAs-like modes. For example, the SQD mode of A_1 symmetry (plotted as an open circle) with $R_\lambda \simeq 20$ Å and nearly the same frequency as the bulk GaAs LO(Γ) phonon is a bulk GaAs-LO(Γ)-like mode, while the SQD mode of A_2 symmetry (plotted as a solid square) with $R_\lambda \simeq 23.5$ Å and frequency slightly above zero, is a surface GaAs-like mode.

In figure 2, we plot the R_λ (Å) as a function of frequency squared for phonon modes in a 10/30 AlAs/GaAs SQD calculated from both the natural charge approach and the neutral charge approach. Figures 2(a) and (b) are results for modes of T_1 and T_2 symmetries, respectively. The data from the natural charge approach are plotted as solid symbols (solid down triangles and solid diamonds), while the data of the neutral charge approach are plotted as open ones. It is seen that small differences are shown by the deviations of open symbols from solid symbols. For the bulk AlAs-like modes (core-interior and core-interface modes having localization radii in the core's interior or near the core's periphery), the solid symbols are shaded totally by the open symbols to indicate the accurate coincidence of both results; however for the shell-interior, shell-interface and shell-surface modes, there are small differences in the coordinates between solid and open symbols, showing the small difference between the GaAs-like modes of the two approaches caused by the small difference in the two kinds of surface charge distribution.

In figure 3, DOSs are evaluated as functions of ν^2 for 30/40, 30/60, 30/80 and 10/80 AlAs/GaAs SQDs, respectively. For comparison, we plot also the GaAs and AlAs bulk-

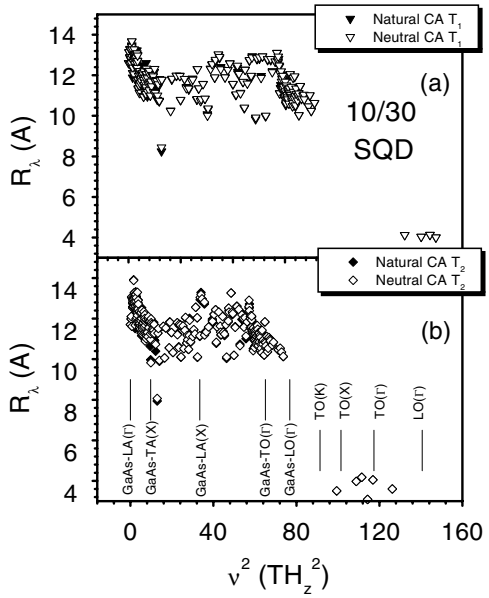

Figure 2. Localization radii of SQD modes of T_1 and T_2 symmetries in a 10/30 AlAs/GaAs SQD. Open symbols and solid symbols are used to denote the data of the neutral charge approach and natural charge approach, respectively.

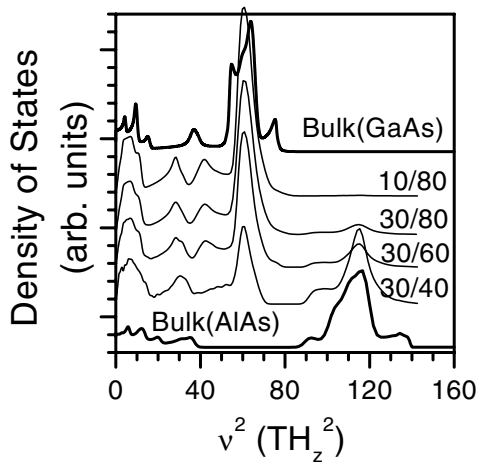

Figure 3. Densities of phonon states of 30/40, 30/60, 30/80 and 10/80 AlAs/GaAs SQDs. DOSs of bulk GaAs and bulk AlAs are also plotted for comparison.

phonon DOSs which are calculated by using 503 special $\boldsymbol{k}$ points in the irreducible BZ. All the DOSs have been broadened by a Gaussian line shape with the half width $\sigma = 0.3$ THz. It is seen that for SQDs with core of fixed size ($d_S = 30$ Å), the DOS becomes more similar to that of bulk AlAs (or bulk GaAs) when the thickness of the GaAs shell decreases (or increases). This results is reasonable because when the thickness of the GaAs shell tends to zero (or to a large value), the SQD becomes nearly a pure AlAs QD (or a pure GaAs QD); it should have a DOS more similar to that of the bulk AlAs (or bulk GaAs). While the DOS of an SQD with

small outer diameter and small shell thickness, the 30/40 SQD for example, is quite different from the bulk GaAs DOS, they become more similar as the size (outer diameter) and shell thickness increase. The DOS of the 10/80 SQD has shown the main characteristics of the bulk-GaAs DOS. Obvious differences remain in that the small peak at about $\nu^2 = 42$ THz^2 in the DOS of the SQD moves to about 37 THz^2 in the DOS of bulk GaAs. The small peak at about $\nu^2 = 78$ THz^2 in the DOS of bulk GaAs is smeared in that of the SQD, and the peak at about $\nu^2 = 60$ THz^2 in bulk GaAs is much lower than that of the SQD, indicating the presence of dense surface-like modes in the SQD in this area. From figure 1 and through the comparison between the DOS of bulk GaAs and those of SQDs, we can see that surface-GaAs-like SQD modes with bigger localization radius concentrate mainly in frequency regions above bulk A(Γ) ($\nu^2 \gtrsim \nu^2_{\mathrm{A}(\Gamma)}$), around $\nu^2 = 42$ THz^2 and in the central area ($\nu^2 \simeq 52$–60 THz^2) between LA(X) and TO(Γ) of bulk GaAs.

To know the extent to which the SQD eigenmode is derived from the bulk GaAs modes near the specific point in reciprocal space, and then discuss the size effects of these bulk-GaAs-like SQD modes, we evaluate the bulk-GaAs-specific $\boldsymbol{k}$ parentage around specific points in $\boldsymbol{k}$ space, as defined in equations (7) [31, 32]. In this article, attention will mainly be paid to the 'bulk-GaAs-Γ parentage', since it plays a more important role in Raman scattering. The bulk-GaAs-LO(Γ), $T_\lambda(6, \mathbf{\Gamma}, K_{cut})$, and bulk-GaAs-TO(Γ) parentages, $\sum_4^5 T_\lambda(n, \mathbf{\Gamma}, K_{cut})$, are calculated as functions of ν^2 for SQDs with different values of d_S and d_L. It is found that for all kinds of SQD, the maximum bulk-GaAs-LO(Γ) parentages always occur in modes with A_1 symmetry (belong to the A_1 irreducible representation) which will be called the bulk-GaAs-LO(Γ)-like SQD modes, while maximum bulk-GaAs-TO(Γ) parentages always occur in modes with T_1 symmetry which will be called the bulk-GaAs-TO(Γ)-like SQD modes. The bigger the outer diameter (or the shell thickness) of the SQD is, the more the maximum parentage of the bulk-LO(Γ)-like SQD mode of A_1 symmetry exceeds the parentages of modes of other symmetries. Similarly, our results show also that the bigger the outer diameter (or the shell thickness) of the SQD is, the more the maximum parentage of the bulk-GaAs-TO(Γ)-like SQD mode of T_1 symmetry exceeds the parentages of modes of other symmetries. The bulk-GaAs-LO(Γ) parentages of SQD modes of all symmetries are plotted as functions of ν^2 in figure 4 where we have fixed the outer diameter d_L, and increase the thickness of the GaAs shell, from 10 Å (40/50 SQDs), 20 Å (30/50 SQDs) and 30 Å (20/50 SQDs) to 40 Å (10/50 QSDs). As a guide to the eye, we use circles to enclose the data of maximum parentages in each subfigure corresponding to certain shell thickness. As the shell thickness reduces, the frequencies of these bulk-LO(Γ)-like SQD modes red-shift due to the quantum confinement caused by the decreasing of the characteristic scale of the internal quantum well, obeying roughly a rule of $\Delta\nu = -142.044/(d^*)^{1.972}$ for SQDs of $d_L = 50$ Å, where $\Delta\nu$ is the frequency shift relative to the frequency of bulk-GaAs-LO(Γ) phonons in units of THz and d^* is the characteristic scale of the GaAs shell defined as $d^* = 2/(\frac{1}{d_L} + \frac{1}{\Delta d})$.

Bulk-GaAs-LO(Γ) parentages are also calculated and plotted as functions of frequency squared in figure 5 for SQDs of fixed shell thickness of 5 Å (the double thickness $\Delta d = 10$ Å) and different outer diameters d_L, i.e., for SQDs of 10/20, 15/25, 20/30 to 50/60 Å. It is seen this time that the frequencies of bulk-GaAs-LO(Γ)-like modes increase resonantly as d_L increases. When d_L increases from 20 to 30 Å or from 40 to 60 Å, the frequencies of bulk-GaAs-LO(Γ)-like modes increase monotonically; however, when d_L increases from 30 to 40 Å the frequencies of bulk-GaAs-LO(Γ)-like modes decrease. Similar circumstances have been found in GaAs/AlAs SQDs [32] having fixed AlAs shell thickness when the outer diameter d_L increases from about 30 to 50 Å. This swing is attributed to the quantum confinement of the internal quantum well originated from the interface effect owing to the bonding difference between the AlAs and GaAs. In figure 6, the frequencies of bulk-GaAs-LO(Γ)-like modes are

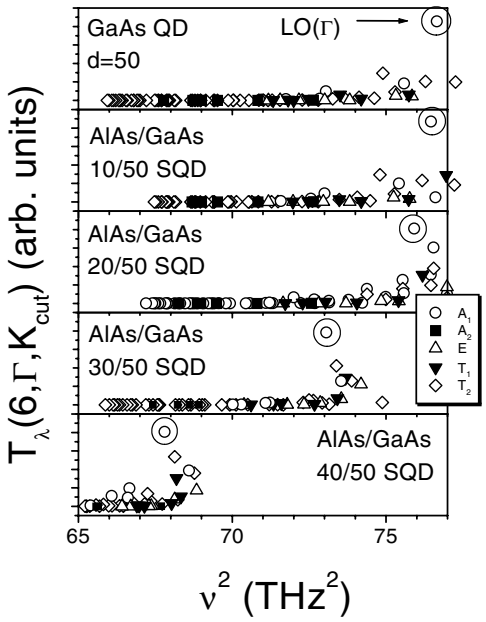

Figure 4. Bulk-LO(Γ) parentage, $T_\lambda(6, \Gamma, K_{cut})$, as a function of ν^2 for phonon modes of each of five symmetries in 10/50, 20/50, 30/50, and 40/50 AlAs/GaAs SQDs as well as in a pure GaAs dot of diameter $d = 50$ Å.

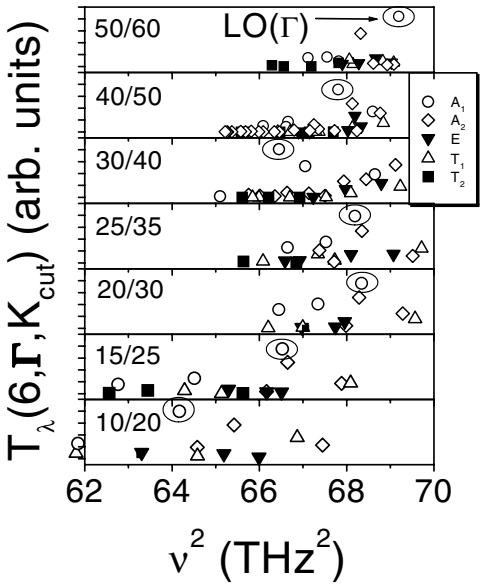

Figure 5. Bulk-LO(Γ) parentage, $T_\lambda(6, \Gamma, K_{cut})$, as a function of ν^2 for AlAs/GaAs SQDs of fixed shell thickness, $\Delta d = 10$ Å, with the outer diameter, d_L as a parameter, i.e., for 10/20, 15/25, 20/30 25/35, 30/40, 40/50 and 50/60 AlAs/GaAs SQDs.

plotted as functions of outer diameters, d_L, for SQDs with different thicknesses. From bottom to top, four curves are given for $\Delta d = 5$, 10, 15 and 30 Å. We see that for all curves with fixed shell thickness, the frequencies of bulk-GaAs-LO(Γ)-like modes increase resonantly as

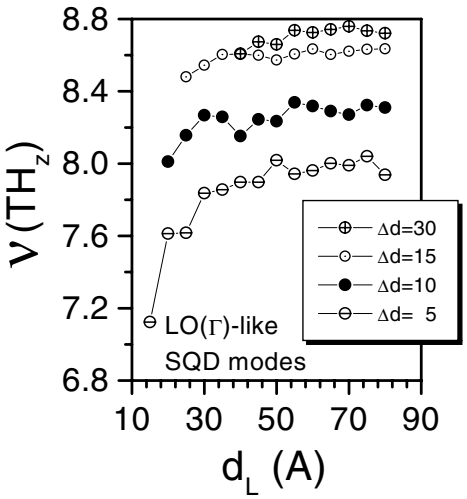

Figure 6. Frequencies of bulk GaAs-LO(Γ)-like SQD modes as functions of the outer diameter of the SQD, d_L, with the shell thickness Δd as a parameter.

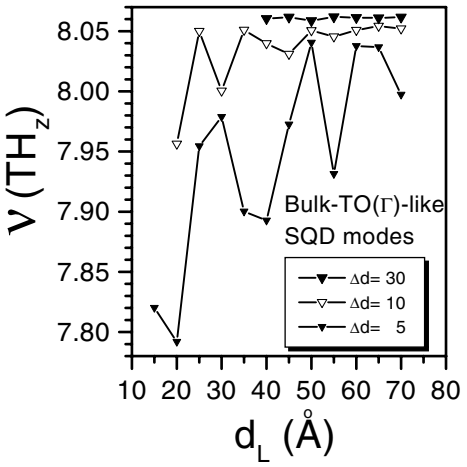

Figure 7. Frequencies of bulk GaAs-TO(Γ)-like SQD modes as functions of the outer diameter of the SQD, d_L, with the shell thickness Δd as a parameter.

d_L increases. However, the smaller the thickness (the narrower the internal quantum well) is, the stronger the quantum confinement effect and so the wider the resonant amplitude will be. Obviously, from figure 6 we can also see the frequency red-shifted effect summarized from figure 5, i.e., for SQDs with the same outer diameter d_L, the frequencies of bulk-GaAs-LO(Γ)-like modes red-shift as the shell thickness decreases.

The frequencies of the bulk-GaAs-TO(Γ)-like modes with T_1 symmetry, i.e., the SQD modes with maximum bulk-GaAs-TO(Γ) parentages, are plotted as functions of d_L in figure 7 with the shell thickness as a parameter. From bottom to top, the three curves give the ν (in THz) versus d_L curves for $\Delta d = 5$, 10 and 30 Å, respectively. As d_L increases, the frequencies of bulk-TO(Γ)-like modes increase resonantly. The thicker the shell is, the wider the waving amplitude will be. For SQDs with fixed d_L, the frequencies of bulk-GaAs-TO(Γ)-

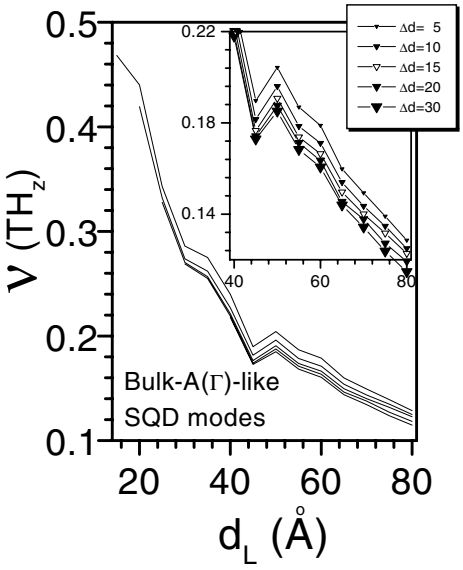

Figure 8. Frequencies of bulk GaAs-A(Γ)-like SQD modes as functions of the outer diameter of the SQD, d_L, with the shell thickness Δd as a parameter.

like modes red-shift as the shell's characteristic scale reduces, roughly obeying a rule of $\Delta\nu = -0.930/(d^*)^{1.508}$ for SQDs of $d_L = 50$ Å. We cannot provide the direct experimental data to confirm the red-shift of bulk-GaAs-TO(Γ)-like and bulk-GaAs-LO(Γ)-like dot modes, but these results are consistent with the shifts of the theoretical Raman peaks in Si QD evaluated by one of the authors [30]. Besides, recently it has been observed by resonant Raman in three samples of Ge nanocrystals in the size range of 4–10 nm that both TO and LO Raman peaks shift to lower frequencies with decreasing dot sizes [39].

We found also that in AlAs/GaAs SQDs, the Γ-derived GaAs acoustic mode, the bulk-GaAs-A(Γ)-like mode (including both LA(Γ) and TA(Γ)) has always T_1 symmetry in all kinds of SQD. In fact, because the lowest frequencies of the AlAs acoustic mode are higher than those of GaAs, the frequency of the bulk-GaAs-A(Γ)-like mode is always the mode of the lowest acoustic frequency in SQDs. The curves of frequencies of bulk-GaAs-A(Γ)-like SQD modes as function of d_L are plotted in figure 8 with the shell thickness as a parameter. From bottom to top five curves of ν versus d_L are given for $\Delta d = 30$, 20, 15, 10 and 5 Å. The inset is an enlarged figure in the region of $d_L = 40$–80 Å. All the data are expressed by open or solid down triangles of which the size is proportional to the thickness of the GaAs shell. It is found that for SQDs with fixed shell thickness, as the size (d_L) decreases, the frequency increases resonantly. Contrary to rules of frequency evolutions of bulk-LO(Γ)-like and bulk-TO(Γ)-like modes, when the outer diameter, d_L, is fixed, the frequencies of the bulk-GaAs-A(Γ)-like mode blue-shift as the shell's characteristic scale reduces, obeying roughly a rule of $\Delta\nu = 0.232/(d^*)^{0.082}$ for SQDs of $d_L = 50$ Å. The origin of the blue-or red-shift of these bulk modes will be revealed below.

In comparison with the results of the GaAs/AlAs SQD given in [29], the main novelty and difference of the phonon spectrum of the AlAs/GaAs SQD is the frequency swing of the bulk-GaAs-like LO(Γ), TO(Γ) and A(Γ) modes in the SQD with definite thickness of GaAs shell as the scale of the SQD increases, as summarized in figures 6–8. There is no such frequency waving of bulk-GaAs-like modes in the GaAs/AlAs SQD.

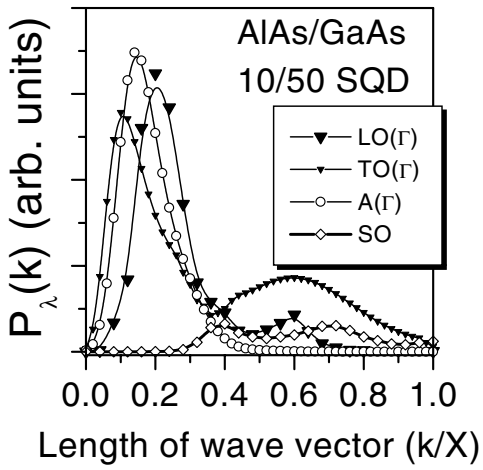

Figure 9. BZ parentages, $P_\lambda(k)$, of the bulklike LO(Γ), TO(Γ), TA(Γ) and surface-like SO modes in a 10/50 AlAs/GaAs SQD.

Then, we discuss the BZ parentage P_λ of the SQD modes defined in equation (6). Figure 9 gives the BZ parentage of three bulklike modes and one SO mode in a 10/50 SQD. It is seen that all three bulklike modes, the TO(Γ)-like, LO(Γ)-like and TA(Γ)-like modes, have a dominant BZ parentage peak around their bulk origin, the Γ point. More accurately, the peak positions of the BZ parentages are located around $|\boldsymbol{k}^*| \simeq 0.13 * (2\pi/a) \simeq 2\pi/d^*$, where $a = 5.65$ Å is the lattice constant of GaAs and $d^* = 2/(\frac{1}{d_L} + \frac{1}{\Delta d}) = 44.\dot{4}$ is the characteristic scale of the GaAs shell. This $\boldsymbol{k}^*$ is just the the quantity used in the 'truncated crystal method' [31, 40]. This approach relates the bulk dispersion $\nu_{n,\boldsymbol{k}}$ to the frequency ν_λ in the SQD, i.e., there exists a k^* that satisfies $\nu_\lambda^{SQD} \simeq \nu_{n\boldsymbol{k}^*}^{bulk}$. In the same figure we plot also the parentage of a surface mode in a 10/50 AlAs/GaAs SQD, i.e., the 32nd mode with maximum localization radius, $R_\lambda = 22.94$ Å, in all 1139 modes of T_2 symmetry and much smaller bulk-Γ parentages in comparison with those of bulklike modes. It is seen that the parentage of the SO mode is delocalized in k space without a sharp peak in the region of $\boldsymbol{k}/\mathrm{X} = 0$–1. Since the frequency of the bulk-GaAs optical modes decreases as $\boldsymbol{k}$ departs from the Γ point, in SQDs the frequencies of the TO(Γ)-like and LO(Γ)-like modes should show a red-shift relative to their bulk values as the characteristic scale reduces. While the frequencies of bulk-GaAs acoustic modes increase as $\boldsymbol{k}$ departs from the Γ point, in SQDs the frequencies of the A(Γ)-like modes should show a blue-shift relative to their bulk values with reducing characteristic scale.

When the size (the outer diameter) of the SQD is small enough, the parentages of the SQD modes with all five symmetries are of nearly the same order of magnitude as can be seen from figure 4, that is a sign of mode mixing due to the quantum confinement of phonon modes. An important example is the LO/TO mode mixing of the phonon modes in SQDs caused by the break of translational symmetry. Table 1 gives the bulk-band parentages defined in equation (8) for modes in several AlAs/GaAs SQDs. It is seen that in the relatively large SQD, the mode mixing is very small. The bulklike SQD modes possess nearly the same main character as bulk modes. However, there exists significant LO/TO mode mixing for surface-like SO modes. The set of A_λ data for the SO mode given in this table is the data of the 69th mode of T_2 symmetry in a 30/50 SQD; this is the mode with maximum localization radius ($R_\lambda \simeq 22.8$ Å) of all T_2 modes, as shown in figure 1 by a solid square at $\nu^2 = 2.071\,35$ THz^2. For this typical surface-like mode, the ratio between $\sum_{n=4}^{5} A_\lambda(n)$(bulk-TO) and $A_\lambda(n = 6)$

Table 1. Bulk-band parentage $A_\lambda(n)$ of bulk-phonon bands (n = 1–6) in forming the LO(Γ), TO(Γ), A(Γ) and SO bulklike SQD modes in SQDs of different sizes.

		$A_\lambda(n)$ (in %)			
Bulklike SQD mode λ	d_S/d_L (Å)	$n = 1+2$ (TA)	$n = 3$ (LA)	$n = 4+5$ (TO)	$n = 6$ (LO)
LO(Γ)	20/50	0.0043	0.3561	2.0084	97.6312
	20/30	0.4358	1.4393	2.7023	95.4226
	10/20	7.7294	3.3777	4.8818	84.0111
TO(Γ)	20/40	8.5603	0.1611	87.6477	3.6309
	20/30	12.5935	0.9124	79.0659	7.4282
	10/20	8.4751	2.4975	67.3964	21.6310
A(Γ)	10/60	59.2914	1.4754	38.4614	0.7718
	20/40	54.4366	4.7433	34.1452	6.6749
SO	30/50	48.7727	1.1979	20.9055	29.1239

(bulk-LO) reaches 0.718. To reveal the relation between mode mixing and the sizes of the SQDs, bulk-band parentages of bulklike modes (n = 1–6) for different sizes of SQDs are also listed. It is seen that in SQDs of small size, the mode mixing is much stronger than in bigger SQDs. For the bulk-TO(Γ)-like dot mode in a 10/20 SQD, the ratio between $A_\lambda(n = 6)$ (bulk-LO) and $\sum_{n=4}^{5} A_\lambda(n)$(bulk-TO) reaches 0.321 in comparison with the value of 0.040 in the 20/40 SQD. Similarly, for the bulk-LO(Γ)-like SQD mode in a 10/20 SQD, the ratio between $\sum_{4}^{5} A_\lambda(n)$ (bulk-TO) and $A_\lambda(n = 6)$(bulk-LO) is 0.058 in comparison with the value of 0.021 in a 20/50 SQD.

Since the phonons of SQDs are derived from bulk phonons, it always helps to understand the SQD phonons from their relations to bulk phonons. In some bulk specimens of zinc-blende semiconductors, such as bulk InAs or GaAs, there is a splitting of the LO and TO at the Γ point due to the long-range Coulomb interaction. Without Coulomb interaction as is the case in bulk Si, the LO and TO modes would be a triply degenerate mode at the Γ point. For $\boldsymbol{k}$ in the [1, 0, 0] and its equivalent directions (six in total and indicated as ⟨1, 0, 0⟩), the phonon spectrum splits into a doubly degenerate $\Delta_3 + \Delta_4$ branch (TO) and a non-degenerate Δ_1 branch (LO); of these two, the Δ_1 branch has a larger dispersion than the $\Delta_3 + \Delta_4$ branch, i.e., the LO frequencies decrease faster than the TO frequencies when the $\vec{k}$ goes away from the Γ point. This is true with or without the Coulomb interaction. For $\vec{k}$ in the [1, 1, 1] and its equivalent directions (four in total, and indicated as ⟨1, 1, 1⟩), the bulk spectrum splits into a doubly degenerate Λ_3 (TO) and a non-degenerate Λ_1 (LO), of which the LO branch has a larger dispersion than the TO branch, with or without the Coulomb interaction. For SQDs with limited size, their frequencies are composed of many bulk states $|n, \vec{k}\rangle$ with $\vec{k} \neq 0$, of which the frequencies are lower than the frequency at the Γ point. Particularly, for the six ⟨1, 0, 0⟩ directions, the linear combination of the LO states $|\Delta_1, \vec{k}\rangle$ gives one A_1 state, one doubly degenerate E state and one triply degenerate T_2 state. We can write this relation as [28]

$$6|\Delta_1, \vec{k}_\Delta\rangle \Rightarrow A_1 + E + T_2. \tag{9}$$

Similarly, for the ⟨1, 0, 0⟩ TO modes we have

$$6|\Delta_3 + \Delta_4, \vec{k}_\Delta\rangle \Rightarrow 2T_1 + 2T_2. \tag{10}$$

For the ⟨1, 1, 1⟩ LO modes we have

$$4|\Lambda_1, \vec{k}_\Lambda\rangle \Rightarrow A_1 + T_2, \tag{11}$$

and for the $\langle 1, 1, 1\rangle$ TO modes we have

$$4|\Lambda_3, \vec{k}_\Lambda\rangle \Rightarrow \mathrm{E} + \mathrm{T}_1 + \mathrm{T}_2. \tag{12}$$

These formulae of resolutions of irreducible representations can indicate in principle the origin of the symmetries of the bulklike SQD modes. Equation (10) explains why the bulk-TO(Γ)-like modes in AlAs/GaAs SQDs are able to have T_1 symmetry, while equation (9) illustrates why the bulk-LO(Γ)-like modes in AlAs/GaAs SQDs are able to have A_1 symmetry.

Our model can in principle deal with the surface reconstruction, because the VFF model based on group theory allows us to deal with the SQDs of which atoms on several atom shells near the surface have different bond length, bond angle and symmetry properties to those of the internal shells. However, until now our preliminary work in this direction has only considered cases in which the atoms located in several surface atom shells have different bond lengths, different bond angles or different masses (in the case of substitution by other kinds of atom), but the same symmetry as the atoms on the internal shells. Our results show that in addition to the change in the number and frequencies of surface modes, the surface reconstruction influences deeply the acoustic modes of very low frequencies. Further details will be given elsewhere.

4. Summary

Phonon modes in spherical AlAs/GaAs SQDs up to about 8.5 nm in diameter are calculated by using the projection operators of the group theory into the VFFM. The phonons of SQD modes in each of five irreducible representations (symmetries) are classified by using a dual-space, the real space and the reciprocal space, analysis method. It is found that the bulklike SQD modes with localization radius located in the interior of the shell or the core have clearly pronounced bulk specific $\boldsymbol{k}$-point parentage, $T_\lambda(n, \boldsymbol{k}_{BZ}, K_{cut})$, from a specific part of the BZ (Γ derived, X derived etc) and from a definite bulk band (one of $n = 1$–6 for TA1, TA2, LA, TO1, TO2 and LO modes). In AlAs/GaAs SQDs of all sizes, each specific bulklike SQD mode has specific symmetry. The bulk GaAs-LO(Γ)-like SQD modes always have A_1 symmetry; the bulk GaAs-TO(Γ)-like and bulk-GaAs-A(Γ)-like SQD modes have T_1 symmetry. The bulklike SQD mode of specific symmetry has a dominant BZ parentage peak around the bulk origins, so the frequencies of these SQD modes can be approximately related to a single bulk phonon band at a single wavevector $\boldsymbol{k}^*$. In addition to the frequencies of bulk GaAs-A(Γ)-like SQD modes blue-shifting as the shell's characteristic scale reduces, the bulk-GaAs-like Γ-derived LO and TO SQD modes red-shift in frequency with decreasing shell characteristic scale. There is almost no LO/TO mixing for bulklike modes. As for the surface-like modes localized at the periphery of the shell or the core, they have no dominant bulk specific $\boldsymbol{k}$-point parentages or dominant BZ parentages around some special points. They are a superposition of many bulk bands with $\boldsymbol{k}$ from all over the bulk BZ. They have much more significant mode mixing than the bulklike phonons. The identification and classification of SQD modes have fundamental importance in the discussion of Raman spectra and electron–phonon interaction as we will discuss in subsequent research.

Acknowledgments

This research is supported by a Special Funds for Major State Basic Research Project of China (G20000683) and the National Science Foundation of China (60176007). SFR is supported by the National Science Foundation of the USA (INT0001313).

References

[1] Ruppin R and Englman R 1970 *Rep. Prog. Phys.* **33** 149
[2] Ruppin R 1991 *Physica* A **178** 195
Ruppin R 1975 *Surf. Sci.* **51** 140
[3] Roca E, Trallero-Giner C and Cardona M 1994 *Phys. Rev.* B **49** 13 704
[4] Chamberlain M P, Trallero-Giner C and Cardona M 1995 *Phys. Rev.* B **51** 1680
[5] Trallero-Giner C, Debernardi A, Cardona M, Menendez-Proupin E and Ekimov A I 1998 *Phys. Rev.* B **57** 4664
[6] Pokatilov E P, Fonoberov V A, Fomin V M and Devreese J T 2001 *Phys. Rev.* B **64** 245328
[7] Canham L T 1990 *Appl. Phys. Lett.* **57** 1046
[8] Zhou S, Honma I, Komiyama H and Haus J W 1993 *J. Phys. Chem.* **97** 895
[9] Mews A, Eychmuller A, Giersig M, Schooss D and Weller 1994 *J. Phys. Chem.* **98** 934
[10] Mews A, Kadavanich A V, Banin U and Alivisatos A P 1996 *Phys. Rev.* B **53** 13 242
[11] Haus J W, Zhou H S, Honma I and Komiyama H 1993 *Phys. Rev.* B **47** 1359
[12] Schooss D, Mews A, Eychmuller A and Weller H 1994 *Phys. Rev.* B **49** 17 072
[13] Bryant G W 1995 *Phys. Rev.* B **52** 16 997
[14] Koberling F, Mews A and Basche T 1999 *Phys. Rev.* B **60** 1921
[15] Pokatilov E P, Fonoberov V A, Fomin V M and Devreese J T 2001 *Phys. Rev.* B **65** 245329
[16] Yoffe A D 1993 *Adv. Phys.* **42** 173
[17] Qin G G and Jia Y Q 1993 *Solid State Commun.* **86** 559
[18] Yeh A T, Cerullo G, Banin U, Mews A, Alivisatos A P and Shank C V 1999 *Phys. Rev.* B **59** 4973
[19] Klimin S N, Pokatilov E P and Fomin V M 1995 *Phys. Status Solidi* b **190** 441
[20] Chamberlain M P, Cardona M and Ridley B K 1993 *Phys. Rev.* B **48** 14 356
[21] Duval E 1992 *Phys. Rev.* B **46** 5795
[22] Klein M C, Hache F, Ricard D and Flytzanis C 1990 *Phys. Rev.* B **42** 11 123
[23] Frohlich H 1949 *Theory of Dielectrics, Dielectric Constant, and Dielectric Loss* (Oxford: Oxford University Press)
[24] Fuchs R and Kliewer K L 1965 *Phys. Rev.* B **140** A2076
[25] Li W S and Chen C Y 1997 *Physica* B **229** 375
[26] Pokatilov E P, Klimin S N, Fomin V M and Devreese J T 2002 *Phys. Rev.* B **65** 075316
[27] Ren S F, Gu Z Q and Lu D Y 2000 *Solid State Commun.* **113** 273–7
[28] Ren S F, Lu D Y and Qin G 2001 *Phys. Rev.* B **63** 195315
[29] Qin G and Ren S F 2001 *J. Appl. Phys.* **89** 6037
[30] Cheng Wei and Ren S F 2002 *Phys. Rev.* B **65** 205305
[31] Fu H, Ozolins V and Zunger A 1999 *Phys. Rev.* B **59** 2881
[32] Qin G and Ren S F 2002 *Commun. Theor. Phys.* at press
[33] Harrison W A 1980 *Electronic Structure and the Properties of Solids* vol 2 (San Francisco, CA: Freeman) p 37
[34] Yu P and Cardona M 1996 *Fundamentals of Semiconductors, Physics and Materials Properties* (Berlin: Springer)
[35] Kunc K, Naalkanski M and Nusimovici M 1975 *Phys. Status Solidi* b **72** 229
Kunc K 1973/74 *Ann. Phys., Paris* **8** 319
[36] Madelung O (ed) 1996 *Semiconductors—Basic Data* 2nd revised edn (Berlin: Springer)
[37] Ren S Y 1997 *Phys. Rev.* B **55** 4665
[38] Ren S Y 1997 *Solid State Commun.* **102** 479
[39] Teo K L, Kwok S H and Yu P Y 2000 *Phys. Rev.* B **62** 1594
[40] Zunger A 1974 *J. Phys. C: Solid State Phys.* **7** 76 629